1521-0111/87/4/697–705$25.00
MOLECULAR PHARMACOLOGY
Copyright © 2015 by The American Society for Pharmacology and Experimental Therapeutics
http://dx.doi.org/10.1124/mol.114.096578
Mol Pharmacol 87:697–705, April 2015

A Renal-Like Organic Anion Transport System in the Ciliary Epithelium of the Bovine and Human Eye

Jonghwa Lee, Mohammad Shahidullah, Adam Hotchkiss, Miguel Coca-Prados, Nicholas A. Delamere, and Ryan M. Pelis

Department of Pharmacology, Dalhousie University, Halifax, Nova Scotia, Canada (J.L., A.H., R.M.P.); Department of Physiology, University of Arizona, Tucson, Arizona (M.S., N.A.D.); and Department of Ophthalmology and Visual Sciences, Yale University, New Haven, Connecticut (M.C.-P.)

Received October 29, 2014; accepted February 6, 2015

ABSTRACT

The purpose of this study was to determine the direction of organic anion (OA) transport across the ciliary body and the transport proteins that may contribute. Transport of several OAs across the bovine ciliary body was examined using ciliary body sections mounted in Ussing chambers and a perfused eye preparation. Microarray, reverse-transcription polymerase chain reaction (RT-PCR), immunoblotting, and immunohistochemistry were used to examine OA transporter expression in human ocular tissues. Microarray analysis showed that many OA transporters common to other barrier epithelia are expressed in ocular tissues. mRNA (RT-PCR) and protein (immunoblotting) for OAT1, OAT3, NaDC3, and MRP4 were detected in extracts of the human ciliary body from several donors. OAT1 and OAT3 localized to basolateral membranes of nonpigmented epithelial cells and MRP4 to basolateral membranes of pigmented cells in the human eye. *Para*-aminohippurate (PAH) and estrone-3-sulfate transport across the bovine ciliary body in the Ussing chambers was greater in the aqueous humor-to-blood direction than in the blood-to-aqueous humor direction, and active. There was little net directional movement of cidofovir. Probenecid (0.1 mM) or novobiocin (0.1 mM) added to the aqueous humor side of the tissue, or MK571 (5-(3-(2-(7-chloroquinolin-2-yl)ethenyl)phenyl)-8-dimethylcarbamyl-4,6-dithiaoctanoic acid; 0.1 mM) added to the blood side significantly reduced net active PAH transport. The rate of 6-carboxyfluorescein elimination from the aqueous humor of the perfused eye was reduced 80% when novobiocin (0.1 mM) was present in the aqueous humor. These data indicate that the ciliary body expresses a variety of OA transporters, including those common to the kidney. They are likely involved in clearing potentially harmful endobiotic and xenobiotic OAs from the eye.

Introduction

Organic anions (OAs) represent a broad class of chemicals that carry a net negative charge at physiologic pH, and include molecules of physiological, toxicological, and pharmacological significance. Systemically, many OAs are eliminated from the plasma via active transport mechanisms in the kidney tubule and hepatocytes. In vivo studies using intravitreal injection of OAs that are actively eliminated from the body, in part by renal tubular secretion, suggest that, in addition to passive elimination via the outflow pathway (Forbes and Becker, 1961), OAs are also eliminated from the eye by active transport. For example, the half-life of carbenecillin (Barza et al., 1982) and iodopyracet (Forbes and Becker, 1960) in the rabbit eye, and cefazolin and carbenecillin in the monkey eye (Barza et al., 1983), increased considerably following concomitant administration of probenecid, a well established inhibitor of renal OA transport. Consistent with the presence of an active OA transport system in the eye, the elimination of iodopyracet from the rabbit eye in vivo was a saturable process with a secretory maximum (Becker and Forbes, 1961). What is not apparent from these early in vivo studies are the ocular tissues that contribute to active OA elimination.

There is considerable in vitro evidence that active transport mechanisms for OAs occur in the anterior uvea (ciliary body and iris). Iris-ciliary body preparations from the rabbit accumulate the OAs iodopyracet (Sugiki et al., 1961), prostaglandin F2α (Bito, 1972), and chlorophenol red (Becker, 1960) in a temperature-dependent and saturable manner, and accumulation is inhibited by metabolic poisons and other OAs (Becker, 1960; Sugiki et al., 1961; Bito, 1972). The well established substrate of the renal OA secretory system, *para*-aminohippurate (PAH), actively accumulates in preparations of monkey ciliary body, with tissue-to-bath ratios of ~6–7 (Stone, 1979). Another substrate of the renal OA secretory system, 6-carboxyfluorescein (6-CF), is preferentially transported in the aqueous humor-to-blood direction across rabbit iris-ciliary body preparations in Ussing chambers (Kondo and Araie, 1994). Together, these in vivo and in vitro data led to the hypothesis that OA transporters present in the kidney are expressed in the ciliary body and that they

This work was supported by the Canadian Institutes of Health Research [Grant 286509] and the Natural Sciences and Engineering Research Council of Canada [Grant RGPIN/418243-2012].
dx.doi.org/10.1124/mol.114.096578.

ABBREVIATIONS: 6-CF, 6-carboxyfluorescein; HRP, horseradish peroxidase; MK571, 5-(3-(2-(7-chloroquinolin-2-yl)ethenyl)phenyl)-8-dimethylcarbamyl-4,6-dithiaoctanoic acid; OA, organic anion; PAH, *para*-aminohippurate; RT-PCR, reverse-transcription polymerase chain reaction; TPD, transepithelial potential difference.

contribute to the active elimination of OAs from the aqueous humor.

The purpose of this study was to determine (1) the direction in which the ciliary body transports OAs; (2) if the ciliary body expresses OA transporters common to other barrier epithelia, including the kidney; and (3) if so, their cellular and subcellular distribution. Expression of 33 OA transporter genes in the ATP-binding cassette and solute carrier families in microdissected human ocular tissues was determined by microarray. The genes examined included OATs, OATPs, NPTs, URAT1, NaDCs, MRPs, BCRP, and P-gp. The OA transporters that were further examined in more detail included OAT1 (SLC22A6), OAT3 (SLC22A8), NaDC3 (SLC13A3), and MRP4 (ABCC4) because they are major components of the renal OA transport system.

Materials and Methods

Reagents and Antibodies. The mouse anti-α1 subunit of Na,K-ATPase monoclonal antibody (clone M8-P1-A3) was obtained from Thermo Scientific (Rockford, IL). The mouse anti-Cx43 monoclonal antibody (clone CX-1B1) was obtained from Life Technologies (Burlington, Ontario, Canada). The rat anti-MRP4 monoclonal antibody (clone M4I-10) used for immunoblotting was obtained from Abcam (Toronto)—this antibody did not work in immunohistochemistry with paraffin-embedded tissues (data not shown), so we used a different antibody for this application. The rabbit anti-MRP4 antibody used in immunohistochemistry was a generous gift from Dr. Frans G. Russel (Radboud University, Nijmegen Medical Centre, Nijmegen, The Netherlands). Details of its synthesis and use in immunolocalizing MRP4 to apical membranes of human proximal tubule has been previously published (van Aubel et al., 2002). The rabbit anti-OAT1 antibody was obtained from Genway Biotech, Inc. (San Diego, CA). The rabbit anti-OAT3 antibody was obtained from Cosmo Bio Co. Ltd. (Tokyo, Japan). The mouse anti-NaDC3 monoclonal antibody (clone 3A6) was obtained from Abnova (Taipei City, Taiwan). The AlexaFluor 488 goat anti-rabbit, AlexFluor 488 goat anti-mouse, horseradish peroxidase (HRP)–conjugated goat anti-rabbit, HRP-conjugated goat anti-mouse, and HRP-conjugated goat anti-rat antibodies, and TRIzol reagent, were obtained from Life Technologies. Normal goat serum (10% solution), 6-CF, and propidium iodide solution (1 mg/ml) were obtained from Life Technologies. The RNeasy Mini Kit was obtained from Qiagen (Valencia, CA). Custom oligonucleotide primers were synthesized by Integrated DNA Technologies (Coralville, IA). [^{3}H]PAH (40–60 Ci/mmol) and [^{3}H]estrone-3-sulfate (50 Ci/mmol) were obtained from American Radiochemicals (St. Louis, MO). [^{3}H]cidofovir (25 Ci/mmol) was obtained from Moravek Biochemicals (Brea, CA). 5-(3-(2-(7-Chloroquinolin-2-yl)ethenyl)phenyl)-8-dimethylcarbamyl-4,6-dithiaoctanoic acid (MK571) was obtained from Sigma-Aldrich (Oakville, Ontario, Canada). Unless noted otherwise, all other reagents and chemicals were from Sigma-Aldrich.

Human Tissues. Human cadaver eyes obtained from the National Disease Resource Interchange (Philadelphia) were used for immunohistochemistry and microarray analysis. Human cadaver eyes used for reverse-transcription polymerase chain reaction (RT-PCR) and immunoblotting were obtained from the Capital Health Tissue Bank (Halifax, Nova Scotia, Canada). All human eyes were processed within <24 hours post enucleation. For RT-PCR and immunoblotting the ciliary processes, retina, retinal pigmented epithelium, iris, and cornea were dissected under a microscope and stored in liquid nitrogen until further analysis. Human kidney cortex from a single donor was obtained from the Eunice Kennedy Shriver National Institute of Child Health and Human Development Brain and Tissue Bank at the University of Maryland (Baltimore, MD). The use of human cadaver eyes was approved by the Research Ethics Board of Dalhousie University and the Human Subjects Committee of Yale University. The use of human kidney tissue was approved by the Research Ethics Board of Dalhousie University. Use of the human cadaver eyes and kidney followed the tenets of the Declaration of Helsinki.

Animal Tissues. Bovine eyes for the Ussing chamber studies and RT-PCR were obtained from W.G. Oulton's & Sons Ltd. (Windsor, Nova Scotia, Canada). Bovine eyes for perfusion were obtained from the University of Arizona abattoir (Tucson, AZ). Use of the bovine eyes was approved by the Dalhousie University Committee on Laboratory Animals and the University of Arizona Institutional Animal Care and Use Committee. Use of bovine eyes conformed to the Association for Research in Vision and Ophthalmology Resolution for the Use of Animals in Ophthalmic and Vision Research.

RNA Isolation, RT-PCR, and Microarray Analysis. Total RNA was isolated using TRIzol reagent and the RNeasy Mini Kit (Qiagen). Samples with RNA integrity number scores above 7.5 were used for expression analysis. RT-PCR was conducted using standard procedures as described previously (Pelis et al., 2009). The oligonucleotide primer sequences used are shown in Table 1. Whole-genome expression profiling was done using the Illumina (San Diego, CA) BeadChip array platform (HumanHT-12 version 4.0 Expression BeadChip Kit). cRNA labeling and hybridization to the chip and array data analysis were carried out by the Yale Neuroscience Microarray Center (NIH Neuroscience Microarray Consortium) at the Keck Foundation at Yale University.

SDS-PAGE and Immunoblotting. Crude homogenates of human ciliary body or human renal cortex were prepared by homogenizing ~0.3 g of tissue using a TissueRuptor (Qiagen) in ~1 ml of

TABLE 1
Oligonucleotide primer sequences used in RT-PCR analysis

Species	Transporter	Oligonucleotide Primer
Human	OAT1	Sense strand: 5′-TCATCTTGAACTACCTGCAGAC-3′ Antisense strand: 5′-CAGAGTCCATTCTTCTCTTGTG-3′
	OAT3	Sense strand: 5′-CTTCGTCTTCTTCCTATCATCC-3′ Antisense strand: 5′-AGACCTAGGGACAGAGAGCTAAG-3′
	NaDC3	Sense strand: 5′-AGTACTTCCTCGACACCAACTT-3′ Antisense strand: 5′-AGTCAAACCACCACTTGAGAG-3′
	MRP4	Sense strand: 5′-ATCTGCTGTCCAATGATGTG-3′ Antisense strand: 5′-CAGTTCGAACAAGTGTCTGC-3′
Bovine	Oat1	Sense strand: 5′-AGCTGGCTCAGTCCTTATACAT-3′ Antisense strand: 5′-GACAGCACCGTAGATAAAGAGAG-3′
	Oat3	Sense strand: 5′-ACAACCTGCTACAGATCTTCAC-3′ Antisense strand: 5′-GATAGCTTATGGCCAGTGTAGTG-3′
	Nadc3	Sense strand: 5′-AGTACTTCCTGGACACCAACTT-3′ Antisense strand: 5′-GTCTCTGTGTTGGGAGCTTTA-3′
	Mrp4	Sense strand: 5′-GATGACATGTACTCGGTGTTTC-3′ Antisense strand: 5′-CTGTAATCAGGTTGTCAAGGAG-3′

ice-cold homogenization buffer containing 300 mM sucrose, 1 mM ethylenediaminetetraacetic acid, and protease inhibitors [in micromolar concentrations: 4-(2-aminoethyl)benzenesulfonyl fluoride hydrochloride, 104; aprotinin, 0.08; leupeptin, 2; bestatin, 4; pepstatin A, 1.5; E-64, 1.4]. The final concentration of crude membrane protein was 2–5 μg/ml. The crude membrane protein was diluted with an equal volume of 2× Laemmli sample buffer containing 2.5% β-mercaptoethanol (final concentration). Except for immunodetection of MRP4, all samples were heated to 100°C for 5 minutes. Standard procedures were used for gel electrophoresis and immunoblotting. The final concentrations of the antibodies were as follows: rabbit anti-OAT1 (5 μg/ml), rabbit anti-OAT3 (1 μg/ml), rat anti-MRP4 (1.5 μg/ml), mouse anti-NaDC3 (0.5 μg/ml), and HRP-conjugated secondary antibodies (0.4 μg/ml). The SuperSignal West Femto chemiluminescent substrate (Thermo Scientific) was used for immunoreactivity detection.

Immunohistochemistry. All immunohistochemistry procedures, including tissue fixation, were nearly identical to those described previously (Pelis et al., 2009). The final concentration of antibodies used for immunohistochemistry were as follows: rabbit anti-MRP4 (1:500 dilution; protein concentration unknown), mouse anti-Cx43 (6.75 μg/ml), mouse anti-Na,K-ATPase (7.28 μg/ml), rabbit anti-OAT1 (1 μg/ml), rabbit anti-OAT3 (5 μg/ml), and Alexa 488–conjugated secondary antibodies (4–10 μg/ml). Nuclei were stained with propidium iodide (5 μg/ml). Immunoreactivity was visualized using a Zeiss LSM 510 META laser scanning confocal microscope at the Cellular and Molecular Digital Imaging facility in the Faculty of Medicine at Dalhousie University.

Ussing Chamber Experiments. Following dissection, bovine ciliary body wedges were mounted in the Ussing chambers with an aperture size of 0.12 cm^2. It was possible to obtain approximately six wedges from a single ciliary body. Each hemichamber contained 1.2 ml of Kreb's solution containing (in mM): 117 NaCl, 4.6 KCl, 20 $NaHCO_3$, 6 mM glucose, 1 mM $MgCl_2$, 1.5 mM $CaCl_2$, and 10 mM HEPES, pH 7.4. The buffer inside the chambers was continuously stirred with magnetic stir bars, gassed with 95% O_2/5% CO_2, and the temperature was maintained at 37°C. Ag/AgCl electrodes were used to monitor the transepithelial potential difference (TPD) and as short-circuiting electrodes. Electrode asymmetry was corrected at the beginning and end of each experiment with fluid resistance compensation. Transepithelial resistance was determined by the change in the TPD generated by a brief 10 μA pulse controlled by a high-impedance automatic dual voltage clamp (DVC 4000; World Precision Instruments, Sarasota, FL). Transepithelial electrical data were collected and analyzed using a PowerLab 28T and LabChart software, respectively (ADInstruments, Colorado Springs, CO).

All transport experiments were conducted under voltage-clamped conditions. Flux measurements began following the addition of

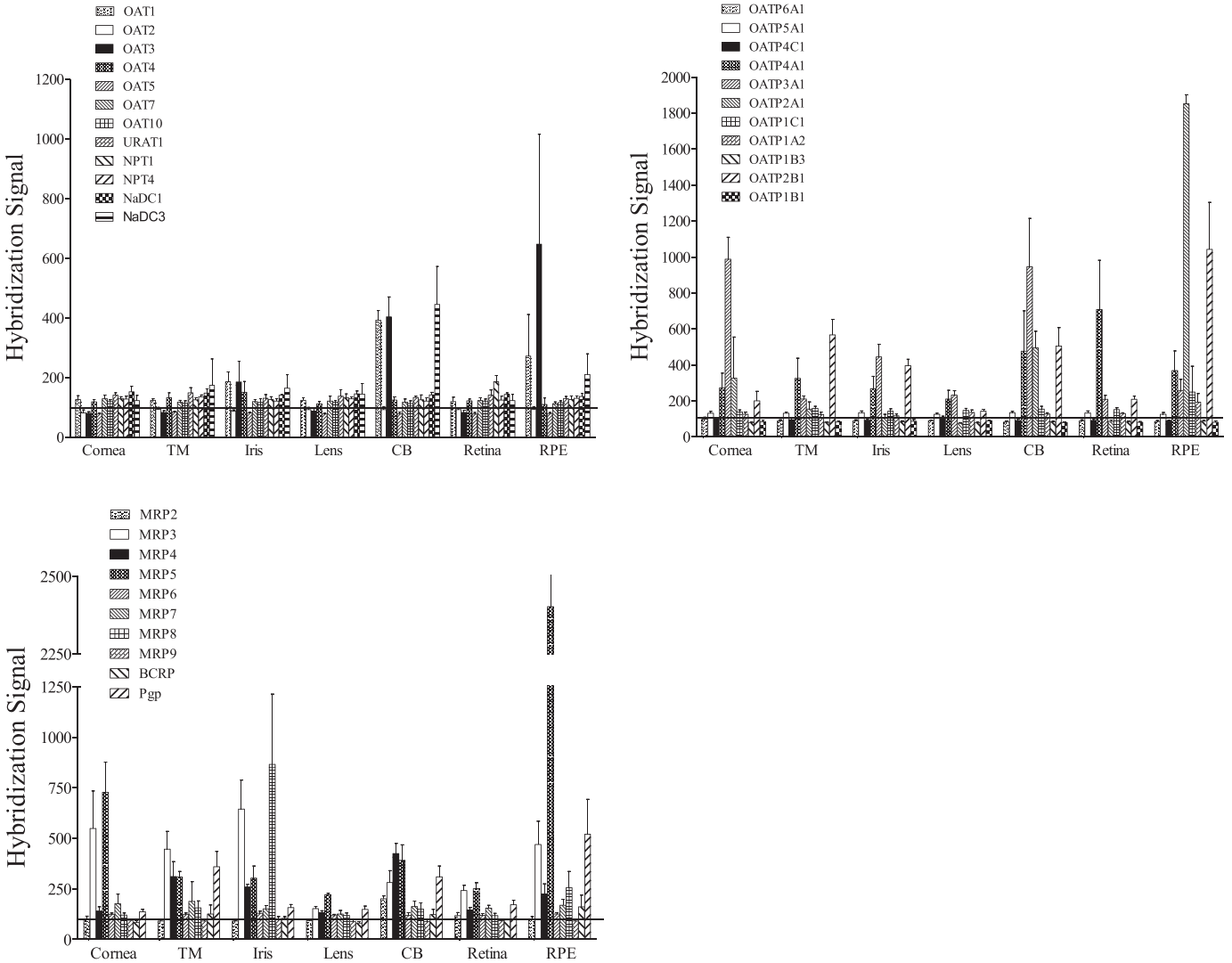

Fig. 1. Microarray analysis of OA transporter expression in microdissected human ocular tissues. The data are the mean ± S.E. of the mean of the hybridization signal from tissue from 5 to 6 individual human donor eyes. The horizontal line represents a background level of the hybridization signal, i.e., only the values above this line are considered a positive signal. TM, trabecular meshwork; CB, ciliary body; RPE, retinal pigmented epithelium.

20–50 nM of ^{3}H-labeled compound (PAH, estrone-3-sulfate or cidofovir) to the appropriate hemichamber (aqueous humor side or blood side), along with a higher concentration of unlabeled compound (5 μM, 15 μM, or 1 mM final concentration, as given in the legends of figures 6, 7, and Table 2) added to both hemichambers. In some cases, probenecid or novobiocin (100 μM final concentration) was added to the aqueous humor side of the tissue, or MK571 (100 μM final concentration) was added to the blood side. Samples were collected at 30 minute intervals over a period of 2 hours. Radioactivity content in the samples was determined by liquid scintillation spectroscopy (LS6500 Scintillation Counter; Beckman Coulter, Brea, CA). For an individual replicate, control and transport protein inhibitor–treated tissues were prepared from the same ciliary body and the flux measurements were performed simultaneously. The TPD and transepithelial resistance were determined at the beginning and end of each experiment to monitor tissue viability.

Perfused Bovine Eye. Bovine eyes were perfused using a method described in earlier studies on aqueous humor formation and multifocal electroretinogram (Shahidullah et al., 2003, 2005). The ophthalmic artery was cannulated and the eye perfused with a physiologic saline. The arterial pressure was continuously monitored using a digital pressure transducer (Model 60-3003; Harvard Apparatus, South Natick, MA) and never exceeded 140 mm Hg. After establishing steady-state perfusion and intraocular pressure (described subsequently) the anterior chamber was cannulated with three 23G needles. The first needle was connected via fine silicon tubing (0.5 mm i.d.) passing through a Watson-Marlow (Wilmington, MA) peristaltic pump to the inlet of a 95 μl quartz flow-through cell. The outlet of the flow-through cell was then connected to the anterior chamber via silicon tubing and to a second 23G needle to constitute the anterior chamber circulating system. The anterior chamber circulating system was filled with aqueous humor substitute containing (in mM): 110 NaCl, 3 KCl, 1.4 $CaCl_2$, 0.5 $MgCl_2$, 0.9 KH_2PO_4, 30 $NaHCO_3$, 6 glucose, and 3 ascorbic acid, equilibrated with 95% O_2:5% CO_2, pH 7.56. The aqueous humor substitute contained either 150 μM of 6-CF (control eyes) or 150 μM 6-CF plus 150 μM novobiocin (treated eyes). Based on the anterior chamber volume of bovine eyes the final concentration of 6-CF and novobiocin in the anterior chamber was ~100 μM. A third needle connected to the anterior chamber continually monitored intraocular pressure, which ranged between 9 and 15 mm Hg at steady state. The aqueous humor compartment was perfused for 150 minutes. After 30 minutes of perfusion the venous effluent (about 1 ml) was collected every 5 minutes. The fluorescence in the samples was read at excitation and emission wave lengths of 492 and 517 nm, respectively, using a Varioskan flash multimode plate reader (Thermo Scientific, Barrington, IL). The amount of 6-CF in the venous effluent was quantified from a standard curve.

Statistics. Data are the mean ± S.E. of the mean. Comparison of sample means was done using an unpaired Student's t test. All statistical analysis was performed with GraphPad Prism (version 5; GraphPad Software, La Jolla, CA) and deemed significant when $P < 0.05$.

Results

Expression of 33 genes corresponding to major OA drug transporters in the SLC and ABC transporter families was determined by microarray in the following microdissected ocular tissues: cornea, trabecular meshwork, iris, lens epithelium, ciliary body, retina, and retinal pigmented epithelium (Fig. 1). The transporters examined were the OATs, URAT1, NPTs, NaDCs, MRPs, BCRP, P-gp, and OATPs. Many of the transporters examined were expressed in the various ocular tissues examined (Fig. 1). We further focused on the expression of OAT1, OAT3, NaDC3, and MRP4 in the ciliary body since the microarray data suggested that (1) the transporters are present; (2) they are primary components of the renal OA transport system (Pelis and Wright, 2011); and (3) previous in vivo and in vitro functional studies showed OA transport activity consistent with their expression in the ciliary body (see *Introduction*).

RT-PCR was further used to examine the mRNA expression of MRP4, NaDC1, NaDC3, OAT1, and OAT3 in the ciliary body, retina, iris, retinal pigmented epithelium, and cornea from a single human donor. All of the tissues examined expressed the α1 subunit of Na,K-ATPase, MRP4, and NaDC3, whereas the other proteins were differentially expressed (Fig. 2). NaDC1 mRNA was only detected in the retina; OAT1 mRNA was detected in the ciliary body, iris, and retinal pigmented epithelium; and OAT3 mRNA was detected in the ciliary body, and to a lesser extent in the retinal pigmented epithelium.

RT-PCR and immunoblotting for OAT1, OAT3, MRP4, and NaDC3 were conducted for additional evidence of their expression in human ciliary body using preparations from four separate human donors—human renal cortex was used as a positive control in each case. mRNA transcripts for OAT1, OAT3, MRP4, and NaDC3 were detected in all human donor samples and in human kidney (Fig. 3). Proteins for OAT1, OAT3, MRP4, and NaDC3 were also detected in ciliary body of all donors examined, as well as in human renal cortex (Fig. 4). OAT1, OAT3, MRP4, and NaDC3 migrated on the SDS-PAGE gels with apparent sizes of ~60, ~60, ~160, and ~55 kDa, respectively.

Immunohistochemistry was used to determine the cellular and subcellular expression pattern of OAT1, OAT3, MRP4, and NaDC3 in paraffin-embedded sections of human eye (Fig. 5). The α1 subunit of Na,K-ATPase served as a marker of basolateral membranes of pigmented cells and nonpigmented epithelium, while Cx43 was used as a marker of apical membranes of pigmented cells and nonpigmented epithelium. The level of immunoreactivity for Na,K-ATPase was high in the

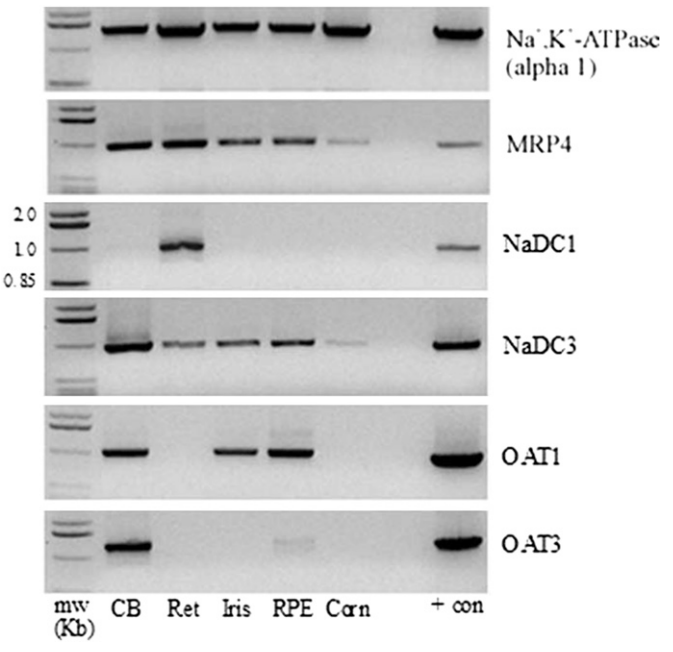

Fig. 2. RT-PCR analysis of Na,K-ATPase (α1 subunit), MRP4, NaDC1, NaDC3, OAT1, and OAT3 in human ciliary body (CB), retina (Ret), iris, retinal pigmented epithelium (RPE), and cornea (Corn). Kidney was used as a positive control. Polymerase chain reaction products were separated on 1% agarose gels and visualized with ethidium bromide. + con, positive control.

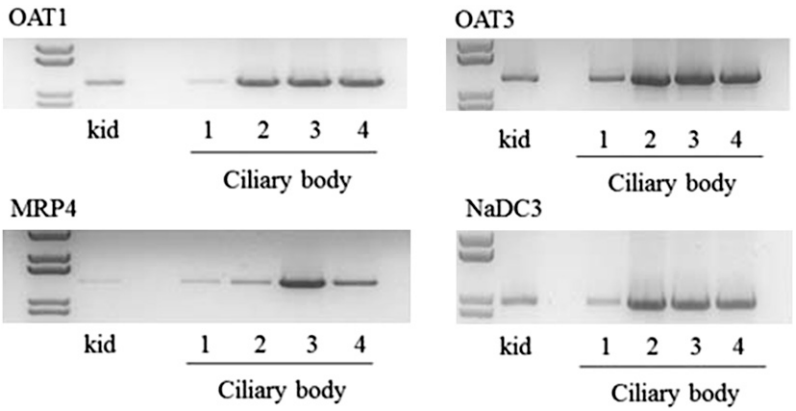

Fig. 3. RT-PCR analysis showing MRP4, NaDC3, OAT1, and OAT3 mRNA transcripts in ciliary body from four separate human donors (1–4). Human kidney cortex was used as a positive control (kid). Polymerase chain reaction products were separated on 1% agarose gels and visualized with ethidium bromide.

basolateral membrane of nonpigmented cells and much weaker (almost undetectable) at the basolateral membrane of pigmented cells. Cx43 had a punctate staining pattern that was sporadic and occurred at the apical junction of pigmented and nonpigmented cells. The pattern of Na,K-ATPase and Cx43 immunoreactivity in the ciliary body is consistent with previous reports (Flügel and Lütjen-Drecoll, 1988; Shahidullah and Delamere, 2014). OAT1 appeared to occur predominately in nonpigmented epithelial cells, with an expression pattern that was consistent with its occurrence in basolateral membranes. OAT3 also appeared to localize to basolateral membranes of nonpigmented epithelial cells. In contrast, MRP4 had a localization pattern consistent with its expression in basolateral membrane of pigmented cells. Attempts to immunolocalize NaDC3 in human ciliary body were unsuccessful.

PAH is a well established substrate of the renal OA transport system. To determine if the ciliary body supports active PAH transport we measured the transepithelial transport of PAH under short-circuited conditions across the freshly dissected bovine ciliary body in the Ussing chambers. Figure 6A shows a representative flux experiment with 1 mM PAH bathing both sides of the tissue. The unidirectional aqueous humor-to-blood flux was greater than the blood-to-aqueous humor flux, with net active transport in the aqueous humor-to-blood direction—net active transport approached steady state at the 2 hour time point. In several different experiments the aqueous humor-to-blood flux was 5.3-fold higher at $t = 2$ hours than the blood-to-aqueous humor flux (Fig. 6B). The TPD and short-circuit current, I_{sc}, values for these control experiments were $66.8 \pm 5.9\ \Omega \times cm^2$, -0.32 ± 0.2 mV (aqueous humor side negative), and $-19.9 \pm 4.2\ \mu A/cm^{-2}$, respectively. The transepithelial electrical properties determined here are in relatively good agreement with previous results (To et al., 1998). We also examined PAH transport at a bath concentration of 5 μM. Under these conditions the aqueous humor-to-blood flux (1.05 ± 0.08 nmol/cm^{-2} per hour^{-1}) was 11.7-fold higher than the blood-to-aqueous humor flux (0.09 ± 0.02 nmol/cm^{-2} per hour^{-1}) at $t = 2$ hours ($n = 3, P < 0.001$, two-tailed unpaired Student's t test). Similar to the human ciliary body, mRNA for Oat1, Oat3, Nadc3, and Mrp4 was detected in bovine ciliary body extracts by RT-PCR using oligonucleotide primers specific for the bovine orthologs of the transporters (Fig. 6C).

Given the evidence for active PAH transport across the bovine ciliary body we also performed inhibition experiments using the well known OA transport inhibitors probenecid, novobiocin, and MK571. Probenecid and novobiocin were added to the aqueous humor side of the tissue only because OAT1, which transports PAH and is inhibited by probenecid (Ingraham et al., 2014) and novobiocin (Duan and You, 2009), localized to basolateral membranes of nonpigmented epithelial cells (Fig. 5). MK571 was added to the blood side of the tissue only to target MRP-mediated efflux—both MRP2 (Pelis et al., 2009) and MRP4 (Fig. 5) localize to the blood side of the ciliary body epithelium. PAH is a substrate of both MRP2 and MRP4, both of which are inhibited by MK571 (Smeets et al., 2004). We used a bath PAH concentration of 1 mM given that net transport approached steady state under these conditions, but did not when the bath contained 5 μM PAH (data not shown). Probenecid nearly abolished all net active transport by reducing the aqueous humor-to-blood flux (Table 2). Novobiocin completely inhibited net active secretion, but its effect was due to an apparent simultaneous reduction in the aqueous humor-to-blood flux and an increase in the blood-to-aqueous humor flux (Table 2). MK571 caused a 60% reduction in the aqueous humor-to-blood flux, but had no effect on the blood-to-aqueous humor flux, resulting in a 68% reduction in net active transport (Table 2). None of the inhibitors influenced the transepithelial electrical properties (data not shown).

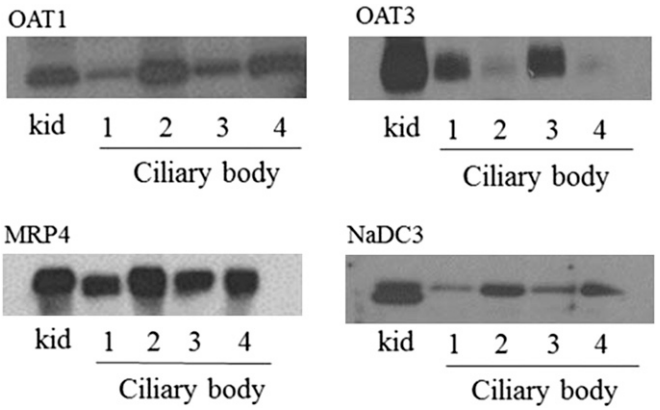

Fig. 4. Immunoblot showing the expression of OAT1, OAT3, and MRP4 in the human ciliary body of four different donors (1–4). Crude homogenate of human kidney cortex served as a positive control (kid). Twenty micrograms of crude homogenate from each of the tissue samples were separated on 4–12% SDS-PAGE gels before electrophoretic transfer of the proteins to polyvinylidene difluoride membranes. Immunoreactivity was detected using protein-specific antibodies and enhanced chemiluminescence detection.

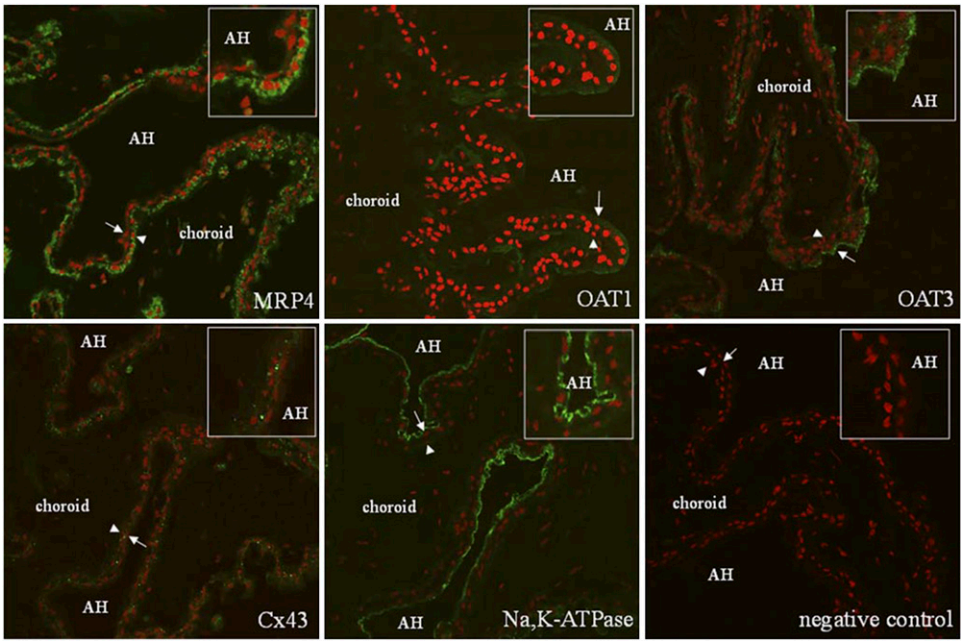

Fig. 5. Immunolocalization of Na,K-ATPase, Cx43, MRP4, OAT1, and OAT3 in paraffin-embedded human eye. Na,K-ATPase was used as a marker of basolateral membranes of pigmented and nonpigmented cells. Cx43 was used as a marker for the apical membrane of both cell types. Proteins of interest are in green and nuclei are stained red with propidium iodide. The arrowheads point to pigmented cells whereas the arrows point to nonpigmented cells. The insets are magnifications of the areas near the arrow and arrowhead. Limited immunoreactivity was detected when the primary antibody was omitted (negative control). AH, aqueous humor.

Since PAH is a preferential substrate of OAT1 versus OAT3 (Zhang et al., 2004), and both the human and bovine ciliary body express OAT3, the transepithelial transport of estrone-3-sulfate (a preferential substrate of OAT3) (Zhang et al., 2004) across the bovine ciliary body in the Ussing chambers was examined. We also examined the transport of cidofovir since it is used clinically to treat cytomegalovirus infections and is an OAT1 substrate (Cihlar et al., 1999). At a bath concentration of 5 μM the estrone-3-sulfate aqueous humor-to-blood flux (26.1 $\pm$ 7.3 pmol/cm^{-2} per hour^{-1}) was 3.5-fold higher than the blood-to-aqueous humor flux (7.45 $\pm$ 1.5 pmol/cm^{-2} per hour^{-1}) at $t = 2$ hours (Fig. 7). Interestingly, there was no significant difference in the unidirectional fluxes of cidofovir across the bovine ciliary body, and net active transport was in the aqueous humor-to-blood direction (Fig. 7).

6-CF was used as a substrate in ex vivo experiments with the perfused bovine eye since it is a substrate of both OAT1 and OAT3 (Rödiger et al., 2010) (and likely other OA transporters as well), and it is actively transported in the aqueous humor-to-blood direction by the ciliary body (Kondo and Araie, 1994). Novobiocin was used as an inhibitor since it inhibits OAT1 and OAT3 (Duan and You, 2009). The amount of 6-CF eliminated from the aqueous humor into the venous perfusate, a product of passive outflow through the trabecular meshwork and flux across the ciliary epithelium, was significantly reduced when novobiocin was present in the aqueous humor (5.78 $\pm$ 0.27 versus 1.19 $\pm$ 0.03 μmol/l^{-1} per hour^{-1}, $P < 0.001$, two-tailed unpaired Student's t test).

Discussion

Gene expression analysis was done to examine OA transporter expression in various microdissected ocular tissues, an approach used previously by others (Zhang et al., 2008; Chen et al., 2013; Dahlin et al., 2013). The transporter expression profiles in the human ciliary body shown in Fig. 1 are in

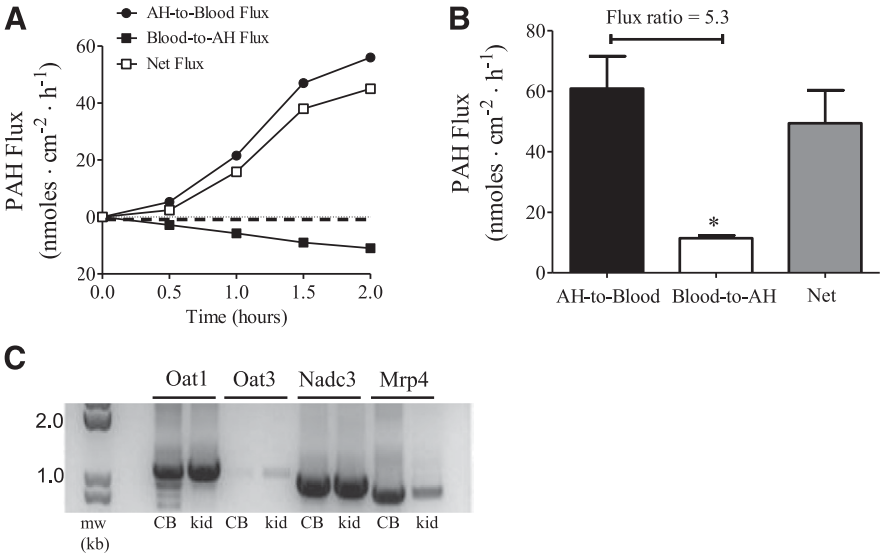

Fig. 6. Unidirectional fluxes [aqueous humor-to-blood (AH-to-blood); blood-to-aqueous humor (blood-to-AH)] and net active flux of PAH across bovine ciliary body in Ussing chambers (A and B). (A) Representative time-course experiment ($n = 1$). (B) Fluxes at steady state ($t = 2$ hours) from four separate experiments (mean $\pm$ S.E. of the mean). The unlabeled concentration of PAH used was 1 mM. Net flux is the difference between the unidirectional fluxes and is in the AH-to-blood direction. *$P < 0.05$, significantly different from the AH-to-blood flux, two-tailed unpaired Student's t test. (C) mRNA expression analysis of Oat1, Oat3, Nadc3, and Mrp4 in the bovine ciliary body (CB) by RT-PCR. Kidney was used as a positive control (kid). Polymerase chain reaction products were separated on 1% agarose gels and visualized with ethidium bromide.

TABLE 2

Effect of probenecid, novobiocin, or MK571 on unidirectional and net fluxes of PAH across the bovine ciliary body in Ussing chambers

The flux values were obtained at t = 2 hours and are the mean ± S.E. of the mean of three separate experiments. The concentration of unlabeled PAH was 1 mM; probenecid and novobiocin were added to the aqueous humor side of the tissue only; MK571 was added to the blood side of the tissue only.

	AH-to-Blood Flux	Blood-to-AH Flux	Net Flux
Control	58.7 ± 10.7	9.4 ± 0.82	49.3 ± 10.2
Probenecid (100 μM)	18.8 ± 3.3[a]	16.9 ± 8.3	1.84 ± 8.2[a]
Control	41.4 ± 10.8	10.8 ± 1.41	30.6 ± 9.4
Novobiocin (100 μM)	28.8 ± 11.1	28.9 ± 15.2	−0.10 ± 4.6[a]
Control	67.6 ± 7.8	16.5 ± 3.6	51.2 ± 10.5
MK571 (100 μM)	26.7 ± 8.7[a]	10.5 ± 1.6	16.2 ± 9.3[a]

AH, aqueous humor.

[a]Significantly different from the control, two-tailed unpaired student's t test; *$P < 0.05$.

relatively good agreement with these previous studies, with a side-by-side comparison shown in Table 3. We further characterized OAT1, OAT3, MRP4, and NaDC3 in more detail since previous in vivo and in vitro functional studies showed OA transport activity consistent with their expression in the ciliary body (see *Introduction*). OAT1, OAT3, NaDC3, and MRP4 were detected in ciliary body preparations from multiple donors by RT-PCR and immunoblotting. OAT1 and OAT3 localized to the basolateral membrane of nonpigmented epithelial cells and MRP4 localized to the basolateral membrane of pigmented cells. We previously showed that MRP2 localizes to the apical membrane of nonpigmented epithelium (Pelis et al., 2009). This is the first study to determine the cellular and subcellular distribution of OAT1, OAT3, and MRP4 in the human ciliary body.

The localization of OAT1 and OAT3 (uptake transporters) on the aqueous humor side of the ciliary epithelium—and the localization of MRP2 and MRP4 (efflux transporters) on the blood side—led to the hypothesis that the tissue would support the transepithelial transport in the aqueous humor-to-blood direction of prototypic substrates of the renal OA transport system. PAH, estrone-3-sulfate, cidofovir, and 6-CF were chosen as substrates since they are all secreted by proximal tubules via the OA transport system (Irish and Dantzler, 1976; Cundy et al., 1995; Shuprisha et al., 1999; Lungkaphin et al., 2006). Net PAH transport across the ciliary body in the Ussing chambers was in the aqueous humor-to-blood direction, and active (voltage-clamped conditions). Consistent with these results, PAH is actively accumulated by in vitro preparations of monkey ciliary body (Stone, 1979). The flux ratio (aqueous humor-to-blood flux/blood-to-aqueous humor flux) was ~2-fold higher at a PAH bath concentration of 5 μM (flux ratio of 11.7) versus 1 mM (flux ratio of 5.3). The decrease in flux ratio with increasing PAH concentration suggests that the rate-limiting step in transepithelial PAH secretion can be saturated—although it was likely not saturated at the 1 mM concentration because the flux ratio was >1 under these conditions. Similar to PAH, the active transport of estrone-3-sulfate across the ciliary body in the Ussing chambers was in the aqueous humor-to-blood direction. In contrast, there was no active transport of cidofovir, i.e., the aqueous humor-to-blood flux and blood-to-aqueous humor flux were not different from each other. Renal tubular secretion of cidofovir is not particularly robust. That is, the renal clearance, CL_R, of cidofovir exceeds the glomerular filtration rate, GFR, but only by a relatively small fraction ($CL_{R,cidofovir}$/GFR ≅ 1.5) (Cundy et al., 1995). Nephrotoxicity is a dose-limiting toxicity for cidofovir in the clinic (Cundy, 1999), largely due to OAT1-mediated uptake of cidofovir into proximal tubule cells (Ho et al., 2000; Uwai et al., 2007); however, perhaps also due to the slow rate at which cidofovir is effluxed from the cells. MRP2 and MRP4, which localize to apical membranes of proximal tubule, do not support ATP-dependent cidofovir transport (Imaoka et al., 2007). The ciliary epithelium generates aqueous humor, which is necessary for maintenance of intraocular pressure. Interestingly, an adverse event associated with cidofovir treatment of cytomegalovirus retinitis is low intraocular pressure (ocular hypotony) (Bainbridge et al., 1999). It is possible that OAT1-mediated cidofovir uptake into ciliary epithelial cells, and its slow rate of cellular efflux, contribute to this adverse event. Probenecid is used to prevent cidofovir-induced nephrotoxicity by blocking OAT1-mediated cidofovir uptake (Cundy, 1999), and may prove useful in ameliorating ocular hypotony in patients receiving cidofovir.

Inhibition studies were done using MK571 to target MRP-mediated efflux, or probenecid or novobiocin to target OA transporter–mediated uptake. MK571 added to the blood side reduced net active PAH transport, likely due to inhibition of MRP-mediated efflux from the ciliary epithelium. Addition of probenecid or novobiocin to the aqueous humor side of the

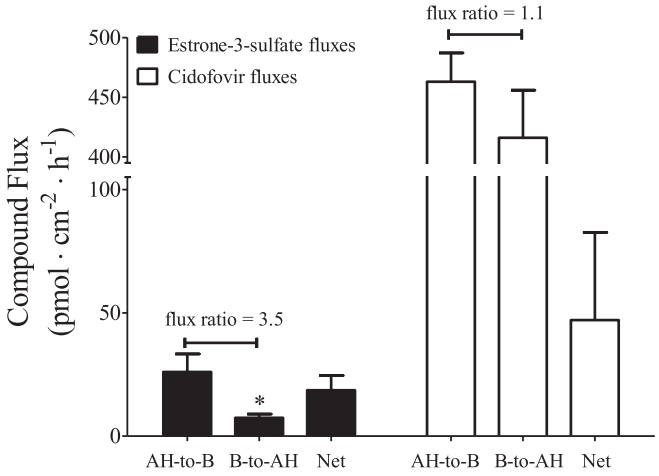

Fig. 7. Unidirectional fluxes [aqueous humor-to-blood (AH-to-B); blood-to-aqueous humor (B-to-AH)] and net active flux of estrone-3-sulfate or cidofovir across the bovine ciliary body in Ussing chambers. The flux values were obtained at t = 2 hours and are the mean ± S.E. of the mean of four (estrone-3-sulfate) or three (cidofovir) separate experiments. The unlabeled concentration of estrone-3-sulfate and cidofovir was 5 μM. The net flux is the difference between the unidirectional fluxes. *$P < 0.05$, significantly different from the AH-to-B flux, two-tailed unpaired Student's t test.

TABLE 3

Comparison of OA transporter genes detected in human ciliary body in this study to three previously published studies

The gene expression data from this study were taken from Fig. 1. The study by Dahlin et al. (2013), as in the present study, used ciliary body, whereas the studies by Chen et al. (2013) and Zhang et al. (2008) used iris-ciliary body preparations. Although Dahlin et al. (2013) examined the expression of other transporters they only reported data for the 10 most highly expressed TransPortal (http://bts.ucsf.edu/fdatransportal) transporter genes identified in their study. The six shown were also examined by us.

Transporter	This Study	Dahlin et al. (2013)	Zhang et al. (2008)	Chen et al. (2013)
OAT1	Detected	—	Detected	—
OAT2	Not detected	—	Not detected	—
OAT3	Detected	—	Detected	—
OATP1A2	Detected (weak signal)	Detected	Not detected	—
OATP1B1	Not detected	—	Not detected	—
OATP1B3	Not detected	Detected	Not detected	—
OATP2B1	Detected	—	Detected	—
MRP2	Detected	—	Not detected	Detected
MRP3	Detected	—	Detected	Not detected
MRP4	Detected	Detected	—	Detected
MRP5	Detected	Detected	—	Detected
MRP7	Detected	—	—	Detected
BCRP	Detected (weak signal)	Detected	Detected	Detected
Pgp	Detected	Detected	Detected	Detected

The em dash (—) indicates that the expression of the transporter gene was not reported or was not examined.

tissue completely abolished net active PAH transport, most likely due to inhibition of OAT1. Probenecid was inhibited by reducing the aqueous humor-to-blood flux. Consistent with the effects of probenecid on transepithelial PAH transport, probenecid inhibited PAH accumulation into monkey ciliary body in vitro (Stone, 1979). The effects of novobiocin were more complex—both unidirectional fluxes appeared to change. The apparent increase in the blood-to-aqueous humor flux caused by novobiocin may reflect the ability of the novobiocin gradient, in the aqueous humor-to-blood direction, to reverse PAH transport via anion exchange mechanisms, which are known to occur in apical membranes of the proximal tubule (Pelis and Wright, 2011). Although the inhibitors were added to one side of the tissue only, we cannot rule out the possibility that the drugs entered the cells and inhibited the pathway at the opposing membrane. Novobiocin was also effective at reducing the rate of 6-CF elimination from the perfused bovine eye. Kondo and Araie (1994) used Ussing chambers to show that 6-CF transport across the rabbit ciliary body, which is in the aqueous humor-to-blood direction (flux ratio ~3), is inhibited by probenecid.

Figure 8 shows a model of OA flux across the ciliary epithelium involving OAT1, OAT3, NaDC3, MRP2, and MRP4. OAT1 and OAT3 occur in basolateral membranes of nonpigmented epithelial cells and operate via a tertiary active transport mechanism to mediate cellular OA uptake. The first step in this process is generation of the Na gradient by Na,K-ATPase, followed by the Na-dependent uptake of α-ketoglutarate (a Kreb's cycle intermediate) by NaDC3. Although we were unsuccessful in immunolocalizing NaDC3 in ciliary body, George et al. (2004) showed by in situ hybridization that NaDC3 mRNA is contained within nonpigmented epithelial cells, where it could occur in either apical or basolateral membranes. Regardless of its localization, it is expected to establish an outwardly directed α-ketoglutarate concentration gradient, thus energizing OA uptake via an exchange mechanism on OAT1 and OAT3. Using the Na,K-ATPase inhibitor ouabain, Kondo and Araie (1994) previously showed that 6-CF transport across the ciliary body in Ussing chambers is Na dependent, which is consistent with the tertiary active uptake mechanism proposed in the present study. Once inside nonpigmented epithelial cells, OAs are pumped across the apical membrane into the intercellular space by MRP2; once in the intercellular space, OAs enter the choroidal blood by diffusing between the leaky junctions between pigmented cells. This is possible since large molecular weight tracers, such as HRP, when injected intravenously, diffuse out of the choroidal blood

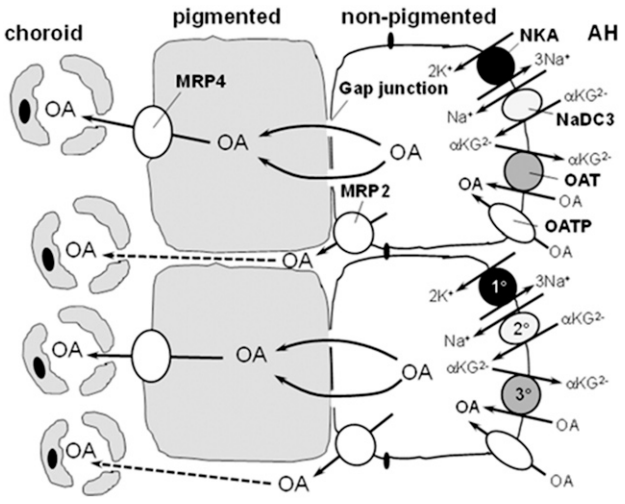

Fig. 8. Hypothetical model of the involvement of NaDC3, OAT1, OAT3, MRP2, and MRP4 in transepithelial OA transport across the ciliary body, aqueous humor (AH)-to-blood (choroid). Uptake of OA across the basolateral membrane of nonpigmented cells occurs via a tertiary active transport process involving Na,K-ATPase (1°; NKA), NaDC3 (2°), and OAT1 and/or OAT3 (3°). OAs are then pumped into the interstitium by MRP2, which localizes to apical membranes of nonpigmented cells. Alternatively, OAs diffuse through gap junctions into pigmented cells and are pumped into the interstitium by MRP4. MRP2 and MRP4 are ATP-dependent efflux transporters. mRNA for NaDC3 has been detected in nonpigmented epithelial cells (George et al., 2004), but its subcellular localization is unknown. It is placed in the basolateral membrane of nonpigmented cells in this model given that it trafficks to basolateral membranes of other epithelial cells. Other OA transporters may also contribute to transepithelial OA secretion. OATPs are included in the model since several OATPs have been localized to the basolateral membrane of nonpigmented epithelium (Gao et al., 2005). The subcellular distribution of other OA transporters in ciliary epithelium is unknown; therefore, they are not included in this model. αKG^{2-}, α-ketoglutarate.

and into the space between adjacent pigmented cells and between the apical junction of pigmented and nonpigmented cells (Freddo, 2001). Alternatively, OAs diffuse through gap junctions connecting nonpigmented and pigmented cells for final efflux into the interstitium by MRP4 located on basolateral membranes of pigmented cells. The currently accepted model for aqueous humor secretion by ciliary epithelium involves the movement of solutes between pigmented and nonpigmented cells through gap junctions (Do and Civan, 2004).

While the proposed model is limited to OAT1, OAT3, NaDC3, MRP2, and MRP4, there are likely other OA transporters functioning in aqueous humor-to-blood flux of OAs. Indeed, the gene expression analysis given here and done by others indicates that the tissue expresses a variety of OA transporters. We previously showed that the human ciliary body expresses protein for P-gp, BCRP, and MRP2, as well as MRP1 (Pelis et al., 2009), and others have shown protein expression for OATP1A2, OATP1C1, OATP2B1, OATP3A1, and OATP4A1 at the basolateral membrane of nonpigmented epithelium in human ciliary body (Gao et al., 2005). Given the tendency for overlap in ligand selectivity of OA transporters, we cannot rule out the possibility that in addition to OAT1, OAT3, MRP2, and MRP4, other OA transporters shown to be expressed in the ciliary body, such as OATPs, MRP1, and BCRP, contributed to transepithelial OA flux across the ciliary body observed here. However, to our knowledge there is no evidence that OATPs or BCRP support PAH transport. In conclusion, the ciliary body expresses a variety of OA transporters, including several involved in renal tubular OA secretion. They are likely involved in clearing OAs from the eye.

Acknowledgments

The authors thank Oulton's Farm (Windsor, Nova Scotia, Canada) and the University of Arizona abattoir (Tucson, AZ) for supplying bovine eyes; Dr. Frans G. Russel of Radboud University, Nijmegen Medical Centre (Nijmegen, The Netherlands), for providing the antibody against MRP4; and the staff at the Capital Health Regional Tissue Bank (Halifax, Nova Scotia, Canada) for assistance with acquiring human donor eyes.

Authorship Contributions

Participated in research design: Lee, Shahidullah, Pelis.

Conducted experiments: Lee, Shahidullah, Hotchkiss.

Contributed new reagents or analytic tools: Coca-Prados, Delamere.

Performed data analysis: Lee, Shahidullah, Pelis.

Wrote or contributed to the writing of the manuscript: Lee, Shahidullah, Pelis.

References

Bainbridge JW, Raina J, Shah SM, Ainsworth J, and Pinching AJ (1999) Ocular complications of intravenous cidofovir for cytomegalovirus retinitis in patients with AIDS. *Eye (Lond)* **13 (Pt 3a)**:353–356.

Barza M, Kane A, and Baum J (1982) The effects of infection and probenecid on the transport of carbenicillin from the rabbit vitreous humor. *Invest Ophthalmol Vis Sci* **22:**720–726.

Barza M, Kane A, and Baum J (1983) Pharmacokinetics of intravitreal carbenicillin, cefazolin, and gentamicin in rhesus monkeys. *Invest Ophthalmol Vis Sci* **24:**1602–1606.

Becker B (1960) The transport of organic anions by the rabbit eye. I. In vitro iodopyracet (Diodrast) accumulation by ciliary body-iris preparations. *Am J Ophthalmol* **50:**862–867.

Becker B and Forbes M (1961) Iodopyracet (diodrast) transport by the rabbit eye. *Am J Physiol* **200:**461–464.

Bito LZ (1972) Accumulation and apparent active transport of prostaglandins by some rabbit tissues in vitro. *J Physiol* **221:**371–387.

Chen P, Chen H, Zang X, Chen M, Jiang H, Han S, and Wu X (2013) Expression of efflux transporters in human ocular tissues. *Drug Metab Dispos* **41:**1934–1948.

Cihlar T, Lin DC, Pritchard JB, Fuller MD, Mendel DB, and Sweet DH (1999) The antiviral nucleotide analogs cidofovir and adefovir are novel substrates for human and rat renal organic anion transporter 1. *Mol Pharmacol* **56:**570–580.

Cundy KC (1999) Clinical pharmacokinetics of the antiviral nucleotide analogues cidofovir and adefovir. *Clin Pharmacokinet* **36:**127–143.

Cundy KC, Petty BG, Flaherty J, Fisher PE, Polis MA, Wachsman M, Lietman PS, Lalezari JP, Hitchcock MJ, and Jaffe HS (1995) Clinical pharmacokinetics of cidofovir in human immunodeficiency virus-infected patients. *Antimicrob Agents Chemother* **39:**1247–1252.

Dahlin A, Geier E, Stocker SL, Cropp CD, Grigorenko E, Bloomer M, Siegenthaler J, Xu L, Basile AS, and Tang-Liu DD et al. (2013) Gene expression profiling of transporters in the solute carrier and ATP-binding cassette superfamilies in human eye substructures. *Mol Pharm* **10:**650–663.

Do CW and Civan MM (2004) Basis of chloride transport in ciliary epithelium. *J Membr Biol* **200:**1–13.

Duan P and You G (2009) Novobiocin is a potent inhibitor for human organic anion transporters. *Drug Metab Dispos* **37:**1203–1210.

Flügel C and Lütjen-Drecoll E (1988) Presence and distribution of Na^+/K^+-ATPase in the ciliary epithelium of the rabbit. *Histochemistry* **88:**613–621.

Forbes M and Becker B (1960) The transport of organic anions by the rabbit eye. II. In vivo transport of iodopyracet (Diodrast). *Am J Ophthalmol* **50:**867–875.

Forbes M and Becker B (1961) The transport of organic anions by the rabbit ciliary body. IV. Acetazolamide and rate of aqueous flow. *Am J Ophthalmol* **51:**1047–1051.

Freddo TF (2001) Shifting the paradigm of the blood-aqueous barrier. *Exp Eye Res* **73:**581–592.

Gao B, Huber RD, Wenzel A, Vavricka SR, Ismair MG, Remé C, and Meier PJ (2005) Localization of organic anion transporting polypeptides in the rat and human ciliary body epithelium. *Exp Eye Res* **80:**61–72.

George RL, Huang W, Naggar HA, Smith SB, and Ganapathy V (2004) Transport of *N*-acetylaspartate via murine sodium/dicarboxylate cotransporter NaDC3 and expression of this transporter and aspartoacylase II in ocular tissues in mouse. *Biochim Biophys Acta* **1690:**63–69.

Ho ES, Lin DC, Mendel DB, and Cihlar T (2000) Cytotoxicity of antiviral nucleotides adefovir and cidofovir is induced by the expression of human renal organic anion transporter 1. *J Am Soc Nephrol* **11:**383–393.

Imaoka T, Kusuhara H, Adachi M, Schuetz JD, Takeuchi K, and Sugiyama Y (2007) Functional involvement of multidrug resistance-associated protein 4 (MRP4/ABCC4) in the renal elimination of the antiviral drugs adefovir and tenofovir. *Mol Pharmacol* **71:**619–627.

Ingraham L, Li M, Renfro JL, Parker S, Vapurcuyan A, Hanna I, and Pelis RM (2014) A plasma concentration of α-ketoglutarate influences the kinetic interaction of ligands with organic anion transporter 1. *Mol Pharmacol* **86:**86–95.

Irish JM, 3rd and Dantzler WH (1976) PAH transport and fluid absorption by isolated perfused frog proximal renal tubules. *Am J Physiol* **230:**1509–1516.

Kondo M and Araie M (1994) Movement of carboxyfluorescein across the isolated rabbit iris-ciliary body. *Curr Eye Res* **13:**251–255.

Lungkaphin A, Lewchalermwongse B, and Chatsudthipong V (2006) Relative contribution of OAT1 and OAT3 transport activities in isolated perfused rabbit renal proximal tubules. *Biochim Biophys Acta* **1758:**789–795.

Pelis RM, Shahidullah M, Ghosh S, Coca-Prados M, Wright SH, and Delamere NA (2009) Localization of multidrug resistance-associated protein 2 in the nonpigmented ciliary epithelium of the eye. *J Pharmacol Exp Ther* **329:**479–485.

Pelis RM and Wright SH (2011) Renal transport of organic anions and cations. *Compr Physiol* **1:**1795–1835.

Rödiger M, Zhang X, Ugele B, Gersdorff N, Wright SH, Burckhardt G, and Bahn A (2010) Organic anion transporter 3 (OAT3) and renal transport of the metal chelator 2,3-dimercapto-1-propanesulfonic acid (DMPS). *Can J Physiol Pharmacol* **88:**141–146.

Shahidullah M, Chan HH, Yap MK, Liu Q, and To CH (2005) Multifocal electroretinography in isolated arterially perfused bovine eye. *Ophthalmic Physiol Opt* **25:**27–34.

Shahidullah M and Delamere NA (2014) Connexins form functional hemichannels in porcine ciliary epithelium. *Exp Eye Res* **118:**20–29.

Shahidullah M, Wilson WS, Yap M, and To CH (2003) Effects of ion transport and channel-blocking drugs on aqueous humor formation in isolated bovine eye. *Invest Ophthalmol Vis Sci* **44:**1185–1191.

Shuprisha A, Lynch RM, Wright SH, and Dantzler WH (1999) Real-time assessment of alpha-ketoglutarate effect on organic anion secretion in perfused rabbit proximal tubules. *Am J Physiol* **277:**F513–F523.

Smeets PH, van Aubel RA, Wouterse AC, van den Heuvel JJ, and Russel FG (2004) Contribution of multidrug resistance protein 2 (MRP2/ABCC2) to the renal excretion of p-aminohippurate (PAH) and identification of MRP4 (ABCC4) as a novel PAH transporter. *J Am Soc Nephrol* **15:**2828–2835.

Stone RA (1979) The transport of para-aminohippuric acid by the ciliary body and by the iris of the primate eye. *Invest Ophthalmol Vis Sci* **18:**807–818.

Sugiki S, Constant MA, and Becker B (1961) In vitro accumulation of chlorphenol red by rabbit ciliary body. *J Cell Comp Physiol* **58:**181–183.

To CH, Mok KH, Do CW, Lee KL, and Millodot M (1998) Chloride and sodium transport across bovine ciliary body/epithelium (CBE). *Curr Eye Res* **17:**896–902.

Uwai Y, Ida H, Tsuji Y, Katsura T, and Inui K (2007) Renal transport of adefovir, cidofovir, and tenofovir by SLC22A family members (hOAT1, hOAT3, and hOCT2). *Pharm Res* **24:**811–815.

van Aubel RA, Smeets PH, Peters JG, Bindels RJ, and Russel FG (2002) The MRP4/ABCC4 gene encodes a novel apical organic anion transporter in human kidney proximal tubules: putative efflux pump for urinary cAMP and cGMP. *J Am Soc Nephrol* **13:**595–603.

Zhang T, Xiang CD, Gale D, Carreiro S, Wu EY, and Zhang EY (2008) Drug transporter and cytochrome P450 mRNA expression in human ocular barriers: implications for ocular drug disposition. *Drug Metab Dispos* **36:**1300–1307.

Zhang X, Groves CE, Bahn A, Barendt WM, Prado MD, Rödiger M, Chatsudthipong V, Burckhardt G, and Wright SH (2004) Relative contribution of OAT and OCT transporters to organic electrolyte transport in rabbit proximal tubule. *Am J Physiol Renal Physiol* **287:**F999–F1010.

Address correspondence to: Dr. Ryan M. Pelis, Department of Pharmacology, Dalhousie University, 5850 College Street, Halifax, NS B3H 4R2, Canada. E-mail: Ryan.pelis@dal.ca